

Enhanced adsorption of methylene blue by citric acid modification of biochar derived from water hyacinth (*Eichornia crassipes*)

Yan Xu^{1,2} · Yunguo Liu^{1,2} · Shaobo Liu^{3,4} · Xiaofei Tan^{1,2} · Guangming Zeng^{1,2} · Wei Zeng^{1,2} · Yang Ding^{1,2} · Weicheng Cao^{1,2} · Bohong Zheng⁴

Received: 12 May 2016 / Accepted: 1 September 2016 / Published online: 10 September 2016
© Springer-Verlag Berlin Heidelberg 2016

Abstract In this work, a novel potential adsorbent, citric acid (CA)-modified biochar, named as CAWB, was obtained from water hyacinth biomass by slow pyrolysis in a N₂ environment at 300 °C. The CA modification focused on enhancing the contaminants adsorption capacity of biochar pyrolyzed at relatively low temperature. Over 90 % of the total methylene blue (MB) could be removed at the first 60 min by CAWB, and the maximum MB adsorption capacity could reach to 395 mg g⁻¹. The physicochemical properties of CAWB was examined by FTIR, XPS, SEM, and BET analysis. The results indicated that the additional carboxyl groups were introduced to the surface of CAWB via the esterification reaction with CA, which played a significant role in the adsorption of MB. Batch adsorption studies showed that the initial MB concentration, solution pH, background ionic strength, and temperature could affect the removal efficiency obviously. The adsorption process could be well described by the pseudo-second-order kinetic model and Langmuir isotherm.

Thermodynamic analysis revealed that the MB adsorption onto CAWB was an endothermic and spontaneous process. The regeneration study revealed that CAWB still exhibited an excellent regeneration and adsorption performance after multiple cycle adsorptions. The adsorption experiments of actual dye wastewater by CAWB suggested that it had a great potential in environmental application.

Keywords Biochar · Water hyacinth · Citric acid · Modification · Adsorption · Dye wastewater

Introduction

Synthetic dyestuffs have been an important class of pollutants, which are extensively utilized in many fields such as textiles, paper, plastic, leather, cosmetics, food processing, wool, and printing (Yagub et al. 2014). The residual dyes in the wastewaters have posed a serious threat to the environment due to their high visibility, recalcitrance, and adverse effects on both the aquatic biota and human health (Mahmoud et al. 2012).

Various physical, chemical, and biological removal techniques such as membrane separation process, coagulation, electrochemical and chemical precipitation, chemical oxidation, and aerobic or anaerobic microbial degradation have been used widely for the decontamination of dyestuffs in wastewater before their release into the environment (Annadurai and Lee 2002). Among these methods, adsorption has been recognized as one of the most effective, versatile, and innocuous technology for the treatment of dye-contaminated effluent (Sun et al. 2013). Activated carbon is often considered to be the most commonly used adsorbent for the decolorization of dyes in wastewater when compared to the other adsorbents such as agricultural solid wastes (Feng et al. 2012), industrial by-products (Gulnaz et al. 2004), and inorganic

Responsible editor: Philippe Garrigues

✉ Yunguo Liu
liuyunguo2012@yeah.net

✉ Shaobo Liu
15171352964@163.com

¹ College of Environmental Science and Engineering, Hunan University, Changsha 410082, People's Republic of China

² Key Laboratory of Environmental Biology and Pollution Control (Hunan University), Ministry of Education, Changsha 410082, People's Republic of China

³ School of Metallurgy and Environmental, Central South University, Changsha 410083, People's Republic of China

⁴ School of Architecture and Art, Central South University, Changsha 410082, People's Republic of China

materials (Auta and Hameed 2012). However, activated carbon is still regarded as an uneconomic adsorbing material due to its expensive sources of raw materials and the high cost associated with its activation process (Yang and Qiu 2010).

Biochar, which has high specific surface area, excellent macroporous structure, enriched functional groups on its surface, as well as a lower cost of feedstocks and production process, appears to be an ingenious alternative to activated carbon (Tan et al. 2015). However, the original biochar still has limited removal ability to the dyes and other contaminants in wastewater, which limits its application to a certain extent. To enhance the adsorption capacity of biochar, many researchers prepared the biochar at high pyrolysis temperature. Mahmoud et al. obtained the kenaf fiber biochar with improved pore structure by HCl treatment after pyrolyzing at 1000 °C, which could be used to remove methylene blue from wastewater (Mahmoud et al. 2012). The iron oxide amended rice husk biochar charred at 950 °C was used to adsorb arsenate due to its high specific surface area in the study of Cope et al. (2014). Harikishore Kumar Reddy and Lee (2014) also prepared a CoFe_2O_4 -modified biochar at 950 °C for Pb^{2+} and Cd^{2+} removal from aqueous solution. In addition, temperatures at 600 °C and above are extensively chosen to prepare the original biochar in many other researches (Burhenne and Aicher 2014; Wang et al. 2013a). Higher pyrolysis temperature may lead to higher adsorption capacity of contaminants onto the biochar by improving the physicochemical properties of biochar like specific surface area, pore structure, and cation exchange capacity (Ahmad et al. 2012). But on the other hand, it could cause the loss of yield and surface functional groups, and higher energy consumption during the preparation, which may diminish the biochar's advantages of cost-effectiveness and resource conservation (Shen et al. 2012). Therefore, it is urgent and necessary to specifically aim at effectively improving the adsorption capacity of the biochar prepared at relatively low temperature.

Citric acid (CA) could be applied to modify the surface of various bioadsorbents by introducing additional carboxyl groups onto their surfaces, which may enhance their dye adsorption capacity (Marshall et al. 1999; Wang et al. 2014; Zhou et al. 2014; Zou and Zhao 2011). Sajab et al. produced CA-modified kenaf core fibers via esterification, which showed higher methylene blue adsorption capacity (131.6 mg g^{-1}) when compared with untreated kenaf core fibers (Sajab et al. 2011). In another research, Zou et al. reported that the CA-treated pine sawdust could be used as an effective adsorbent, of which the methylene blue removal capacity (111.46 mg g^{-1}) could be increased significantly by CA modification (Zou et al. 2013). As for the application of biochar modification, CA could be used as a macropore creating agent in the pretreatment of Zn-modified biochar by fabricating the macropores via thermal decomposition to provide more inner space for ZnCl_2 according to the study conducted

by Kong et al. (2014). As yet, CA has never been used as a surface modification agent impregnated on the surface of the biochar to enhance its adsorption capacity of contaminants by improving the quantity and composition of functional groups.

Water hyacinth (*Eichornia crassipes*), as one of the worst aquatic plants and the most aggressive invasive species in the world, has been a serious problem around the world due to its rapid spread and uncontrolled growth (Malik 2007). The conversion of the biomass of this invasive species into biochar for adsorbing pollutants in water could be a feasible and sustainable strategy for management of water hyacinth (Masto et al. 2013). Methylene blue (MB) is accepted as a model compound for determining adsorption capacity of contaminants, particularly organic dyes onto various adsorbents in liquid-phase adsorption (Zhang et al. 2010). In this study, water hyacinth biomass-derived biochar through slow pyrolysis in a N_2 environment at 300 °C was modified by CA to enhance its adsorption ability for MB from aqueous solution at the first time. A series of laboratory experiments, including characterization experiment and batch sorption experiment, were carried out to investigate the physicochemical properties and MB adsorption mechanisms of the CA-modified biochar. It is our overarching objective of this work to explore a new highly efficient and cost-effective adsorbent with high adsorption capacity, less energy consumption, and low production cost that can be widely utilized in water contaminant removal.

Materials and methods

Materials

All chemicals in this work were of analytical grade without any further treatment. Citric acid was purchased from Tianjin Hengxing Chemical Reagent Co., Ltd. (Tianjin, China). Methylene blue ($\text{C}_{37}\text{H}_{27}\text{N}_3\text{Na}_2\text{O}_9\text{S}_3$) was produced by Sinopharm Chemical Reagent Co., Ltd. (Shanghai, China). MB stock solution was prepared by dissolving it into ultrapure water ($18.25 \text{ M}\Omega \text{ cm}^{-1}$). The working solutions were prepared by diluting the MB stock solution with ultrapure water to certain concentration as required in each experiment. River water was obtained from Xiangjiang River in Changsha, Hunan province, China. The actual dye wastewater with an MB concentration of 236 mg L^{-1} and pH of 8.1 was collected from a textile mill in Changsha, Hunan Province, China.

Preparation of CA-modified biochar

The water hyacinth in this work was obtained from Changsha, Hunan Province, China, and washed with ultrapure water for several times and the stems separated and dried at 60 °C for 48 h. The dry biomass was crushed into powder and then pyrolyzed in a tube furnace at 300 °C with a heating rate of

5 °C min⁻¹ under N₂ atmosphere for 2 h. Two grams of the powered water hyacinth biochar (WB) was added into 100 mL of 0.6 mol L⁻¹ CA solution and stirred at 300 rpm for 2 h at room temperature (25 ± 2 °C). The CA-impregnated biochar was dehydrated at 60 °C for 24 h, then heated to 120 °C and kept for 90 min before cooling down to room temperature. The obtained biochar modified by CA (CAWB) was washed with ultrapure water for several times to remove excess CA and finally dried at 60 °C for 24 h. The detailed preparation process of CAWB described above is shown in Fig. 1.

Characterization of WB and CAWB

Scanning electron microscopy (SEM) (JSM-7001F, Japan) was used to examine the surface morphology of the prepared materials. The surface functional groups on the materials were verified by Fourier transform infrared spectrum (FTIR) (Nicolet 5700 spectrometer). Surface chemical composition of the samples was characterized with an ESCALAB 250Xi x-ray photoelectron spectrometer (XPS) (Thermo Fisher, USA). Brunauer, Emmett, and Teller (BET) analysis was carried out to measure the specific surface area and the pore volume of the samples by using gas (N₂) adsorption-desorption with a gas sorption analyzer (Quantachrome Quadrasorb SI, USA).

Batch adsorption experiments

All the adsorption experiments in this work was conducted by adding 50 mg of the adsorbent to 50 mL of MB solution in a 100-mL conical flask, and the mixture was placed on a mechanical shaker (SHY-2A, China) at 130 rpm for the designated time at the needed temperature. The effect of biochar production temperature on the removal efficiency of MB was studied by adding the adsorbents resulted from different temperatures to 200 mg L⁻¹ MB solutions at pH 10.0, 30 °C for 24 h. The effect of initial MB concentration in the solutions was investigated by mixing CAWB with various concentrations of MB solutions (100, 200, 300, 400, 500, and 600 mg L⁻¹) at pH 10.0 for 24 h. To explore the influence of initial pH of MB solution, 0.1 mol L⁻¹ of HCl and NaOH was used to adjust the initial pH of the solutions. The adsorbent was added to the 300 mg L⁻¹ MB solutions with a series of different pH (2.0, 3.0, 4.0, 5.0, 6.0, 7.0, 8.0, 9.0, 10.0) at 30 °C for 24 h. The effect of ionic strength was studied by adding CAWB to the 200 mg L⁻¹ MB solutions containing different concentrations of NaCl (0.001–0.5 mol L⁻¹) at pH 10.0, 30 °C for 24 h. The samples were filtered to measure the MB concentrations using a UV-vis spectrophotometer (UV-2250; Shimadzu Corporation, Japan) at a wavelength of 665 nm after filtration of the solution.

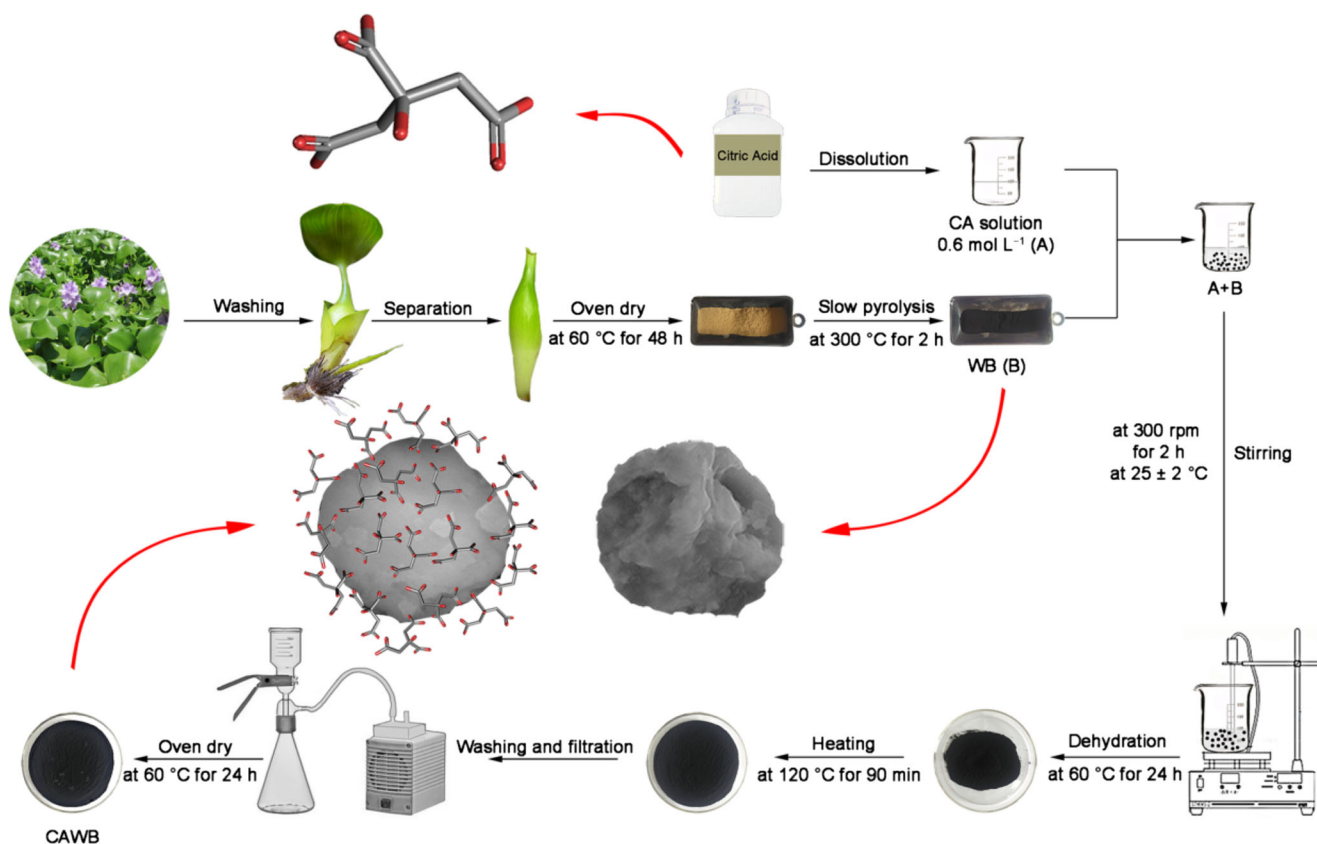


Fig. 1 Scheme for the preparation of CA-modified biochar

Adsorption kinetics of MB onto CAWB were measured with 300 mg L^{-1} at pH 10.0, $30 \text{ }^\circ\text{C}$. The residual concentrations of MB in the solutions were determined at various time intervals (5, 10, 30, 60, 120, 180, 360, 720, 900, 1080, 1440, and 2880 min). MB adsorption isotherms and thermodynamic analysis were achieved at different MB concentrations (50, 100, 200, 300, 400, 500, 600, and 800 mg L^{-1}) at pH 10.0 and at temperatures of 30, 40, and $50 \text{ }^\circ\text{C}$, respectively. The samples were then filtered and the MB concentrations were analyzed spectrophotometrically by the same method. Several sequential adsorption-desorption experiments were conducted to verify the feasibility of regenerating CA-modified biochar. The adsorbent loaded with MB was filtered and washed for several times with ultrapure water to remove unadsorbed MB. The resulting adsorbent was added into 50 mL of 0.1 mol L^{-1} HCl and shaken at 130 rpm under $30 \text{ }^\circ\text{C}$ for 12 h. The regenerated adsorbent was filtered, dried at $60 \text{ }^\circ\text{C}$ for 24 h, and then reused to adsorb MB as described above.

Application of CAWB to real dye wastewater

The study on environmental application of CAWB to actual industrial effluent was investigated by adding 50 mg of CAWB to 50 mL of industrial effluent collected from a textile mill in Changsha and to the MB solutions prepared with ultrapure water and river water with the same MB concentration of 236 mg L^{-1} and the same pH of 8.1 at $30 \text{ }^\circ\text{C}$ for 24 h. The samples were then filtered and the MB concentrations were analyzed by the same method above.

Results and discussion

Characterization of WB and CAWB

FTIR

The FTIR spectroscopy could be utilized to determine the changes in the surface functional groups of the biochar during the CA treatment. The spectra, as seen in Fig. 2, displayed a number of adsorption peaks indicating the complex nature of the adsorbent. It could be obviously found that two new peaks appeared at 1438.7 and 1702.9 cm^{-1} after CA treatment, respectively. The former band was assigned to the stretch vibration of C–O associated with the carboxyl group, indicating that additional carboxyl groups were introduced onto the surface of the biochar by the esterification reaction with CA (Qian and Chen 2014). This hypothesis was confirmed by the latter band which was assigned to the C=O stretch of ester carbonyl group generated in the esterification reaction (Chen et al. 2011a). Furthermore, it could be seen that there existed a significant increase in the intensity of the band at 1621.9 cm^{-1} which was associated with a region of the ionized coordinated

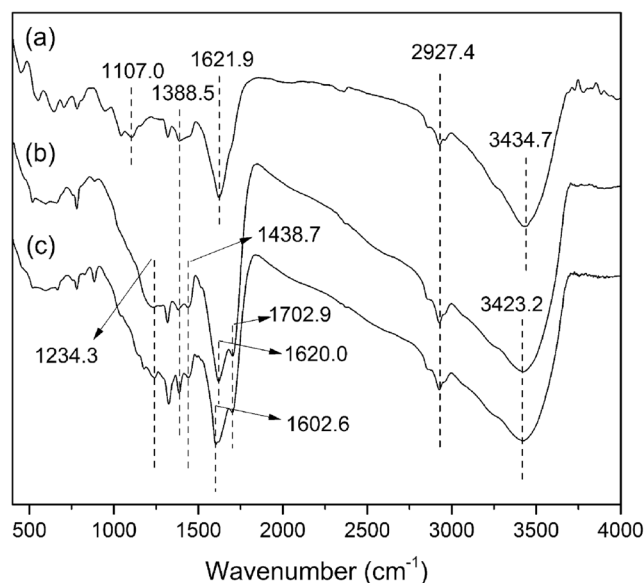


Fig. 2 FTIR spectra of a WB, b CAWB, and c CAWB with MB

and the ionized non-coordinated COO^- group form of the carbonyl from the surface carboxyl group, verifying the introduction of additional carboxyl groups (Dong et al. 2011). The broad adsorption peak at 3434.7 cm^{-1} , which was indicative of hydroxyl vibrations, did not become weak after modification, demonstrating that the introduction of carboxyl groups happened without the cost of decreasing the hydroxyl groups on the biochar surface (Tong et al. 2011). The band at 1107.0 cm^{-1} corresponding to C–O–H asymmetric bending vibration shifted to 1234.3 cm^{-1} which was assigned to C–O–H symmetric bending vibration after the esterification reaction with CA, indicating the change of C–O–H groups during the modification process (Leyva-Ramos et al. 2012).

The FTIR analysis could also reveal the adsorption mechanism involved in the removal of MB by CAWB via comparing the spectrum before and after adsorption. As seen from Fig. 2, there was a little and negligible change between the spectrum a, b, and c at the adsorption peaks located at 1388.5 and 2927.4 cm^{-1} , which corresponded to the bending and stretch vibration of C–H bond, respectively. Nevertheless, it was obvious to find that the 3423.2 and 1620.0 cm^{-1} peaks, corresponding to the hydroxyl group and carbonyl from the carboxyl group of CAWB, shifted to a lower frequency at 3421.3 and 1602.6 cm^{-1} , respectively, with diminished peak intensity after the MB adsorption. These changes may be due to the specific interactions between hydroxyl and carboxyl groups with MB molecules. This analysis result was consistent with previous works (Inyang et al. 2014). Moreover, it could be seen from spectrum c that a new peak appeared at 1492.7 cm^{-1} corresponding to C=N stretching of MB molecule after MB adsorption, verifying that the MB was adsorbed to the surface of CAWB (Low et al. 2004).

XPS

To further understand the changes of the chemical composition on the biochar surface during CA modification, XPS analysis was performed, and the results are shown in Fig. 3. As seen from Fig. 3a, the surface principal element contents such as carbon (C), oxygen (O), and nitrogen (N) of WB were 72.36, 23.08, and 4.56 %, respectively, whereas these element contents of CAWB were 69.51, 26.69, and 3.80 %, respectively, as seen from Fig. 3b. A higher O1s/C1s atomic ratio after modification indicated an increase in the total amount of oxygen-containing functional groups on the surface of CAWB, which may be due to the introduction of carboxyl groups during the CA treatment (Qian and Chen 2014). In addition, the O1s/C1s atomic ratio could be used to reveal the surface hydrophilicity of the carbon material (Chen et al. 2011b), and the higher O1s/C1s atomic ratio of CAWB denoted that it had a higher affinity to water. This might affect the adsorption of aqueous organic contaminants such as MB (Ahmad et al. 2014). Furthermore, Fig. 3c reflected the C1s XPS spectra of WB, which could be well curve-fitted into three peak components at approximately 284.7 eV (C–C), 286.4 eV (C–O), and 287.8 eV (C=O), respectively. The C1s XPS spectrum of CAWB, according to Fig. 3d, could

be deconvoluted into four peaks at the binding energy of 284.8 eV (C–C), 286.5 eV (C–O), 287.8 eV (C=O), and 289.2 eV (O–C=O) (Jing et al. 2014). We could easily find that a new peak appeared at 289.2 eV which was attributed to ester groups after CA modification. This may be owing to the esterification reaction between the hydroxyl groups of the biochar surface and the carboxyl anhydrides dehydrated from CA (Wang et al. 2013b). The proposed modification mechanism mentioned above is displayed in Fig. 4. As seen from Fig. 4, additional carboxyl groups were introduced on the surface of the biochar by the thermochemical reaction of CA with biochar hydroxyl groups, leading to a greater amount of carboxyl groups. This could be verified by the enhanced peak height signal at the binding energy of 287.8 eV in Fig. 3c which represented the C=O in carboxyl groups when compared with Fig. 3d. It should be noted that the further heating may not further increase but cause a detrimental effect on the carboxyl group content due to the additional dehydration and multi-point cross-linking reaction, as demonstrated in Fig. 4 (Wang et al. 2013b). Consequently, the control of reaction conditions such as the temperature and time of the thermochemical reaction are the key parameters to ensure the modified effect during the modification process. These two parameters in the heating process, temperature and time, in this work

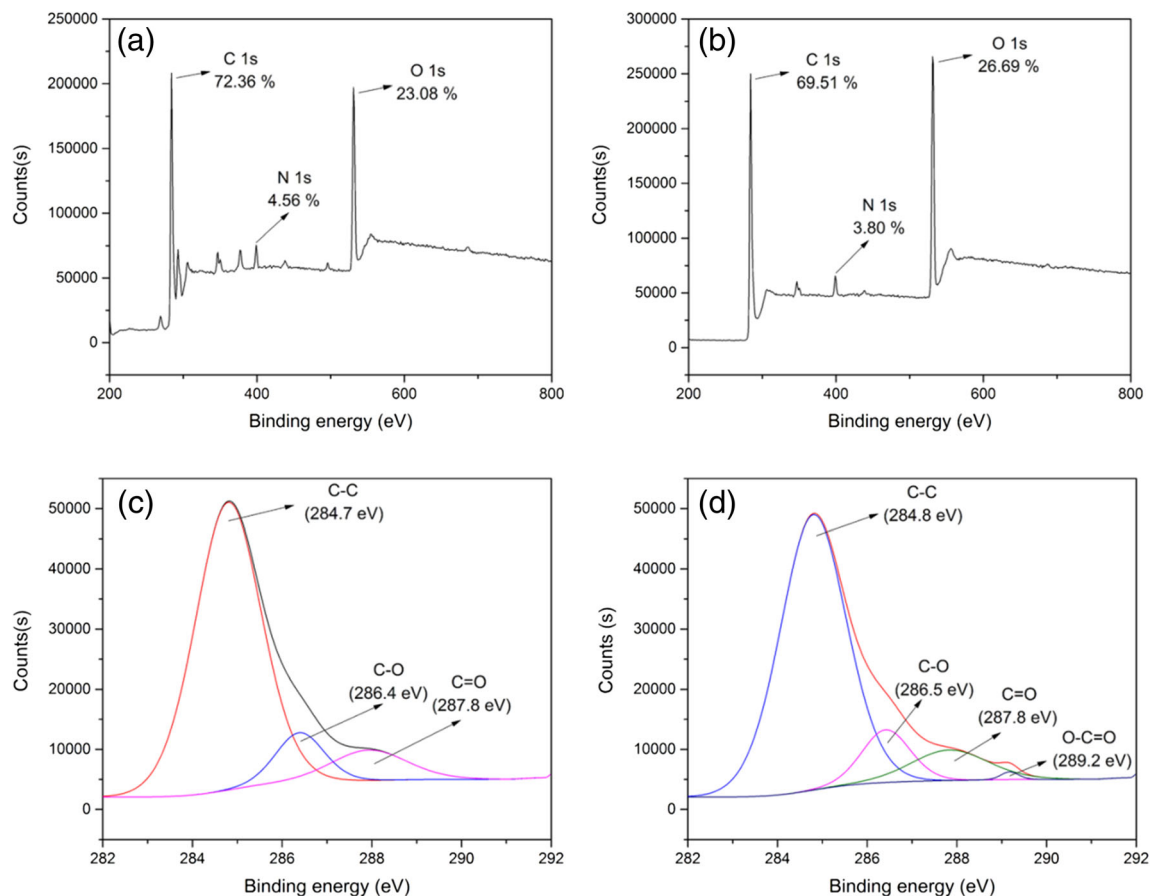


Fig. 3 XPS survey spectra of **a** WB and **b** CAWB; C1s XPS spectra of **c** WB and **d** CAWB

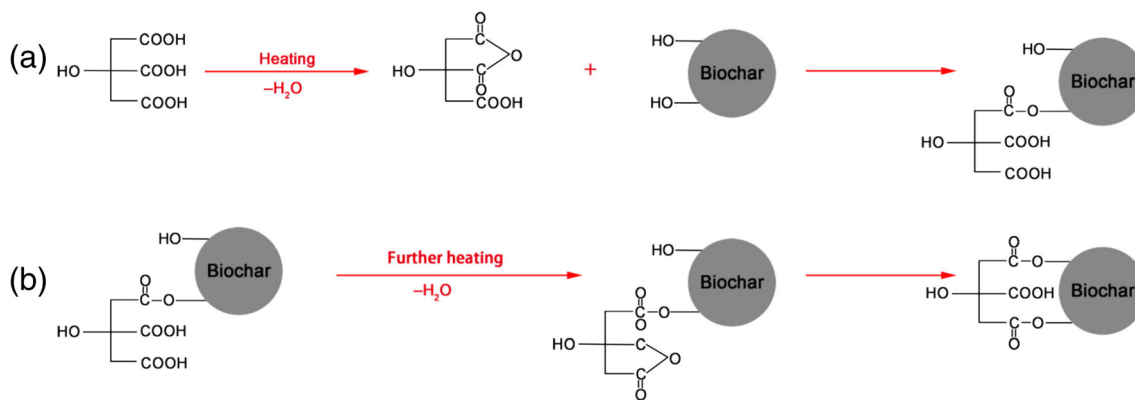


Fig. 4 The proposed mechanism of **a** ideal CA modification of biochar and **b** multi-point cross-linking reaction caused by further heating

were set as 120 °C and 90 min, respectively, which were reasonably selected by conducting several comparison testing and comparing the modified effect in the previous research works (Mao et al. 2010; Wang et al. 2013b).

SEM and BET

The surface morphologies of the pristine biochar (WB) and CA-treated biochar (CAWB) are displayed in the SEM images. Figure 5a reflects that there existed multiple holes on the surface of WB to form a rough and heterogeneous surface, leading to a high surface area of WB. By comparing with Fig. 5b, it could be obviously found that the surface of the material became smoother and more homogeneous after CA modification. Table 1 presents the results of BET analysis, such as specific surface area, total pore volume, and average pore size of the CAWB, which suggested that the CA treatment may cause a detrimental effect to the surface area of the biochar. As could be seen from Table 1, the specific surface area and the total pore volume decreased by 38.6 and 32.6 %, respectively, whereas the average pore size increased from 4.842 to 5.319 nm. The residual organic matter such as lignin after pyrolysis at 300 °C could be solubilized and washed off by CA during the CA treatment, which could account for the increase in the average pore size and the change in surface morphology before and after CA treatment (Kong et al. 2014). The specific surface area and the total pore volume did not increase with the enhancement of the average pore size due to the pore blockage by adsorbed CA molecules which have a small molecular size and could easily access the pore structure of the biochar (Chen et al. 2003). Therefore, N₂ has less affinity during its sorption process, leading to a reduced data of surface area and pore volume of CAWB compared to WB. This was consistent with the studies reported by Chen et al. (2003) and Pitsari et al. (2013). It should be noted that the adsorption capacity of MB onto CAWB did not decrease but was

significantly improved after CA treatment due to the introduction of carboxyl group on the surface of the biochar. This result may indicate that the functional groups play a more important role than specific surface area in the MB adsorption process.

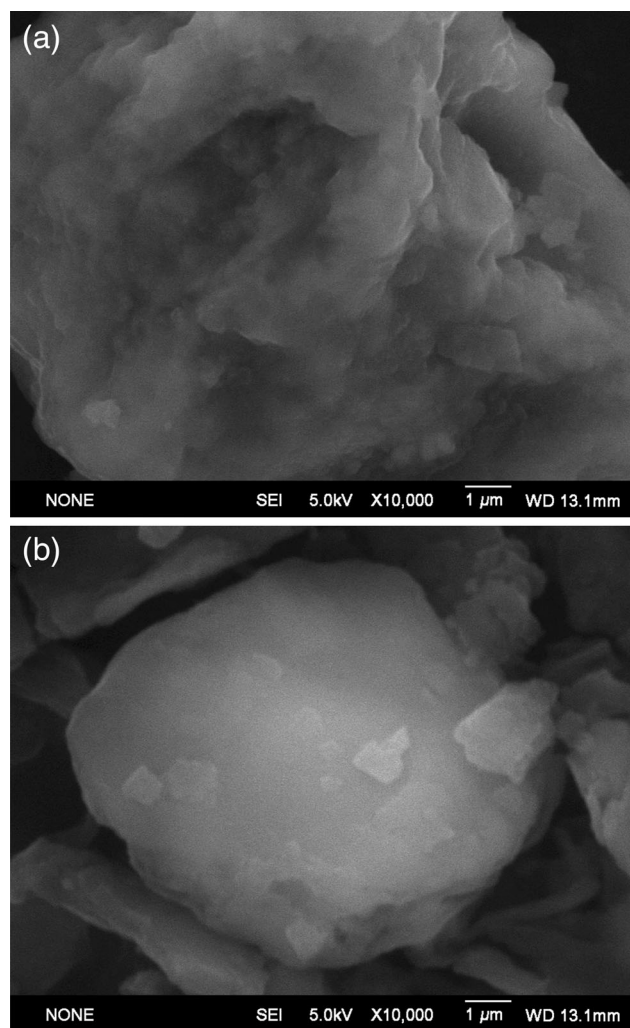


Fig. 5 Scanning electron micrographs of **a** WB and **b** CAWB

Table 1 BET analysis parameters of WB and CAWB

	Specific surface area ($\text{m}^2 \text{g}^{-1}$)	Pore volume ($\text{cm}^3 \text{g}^{-1}$)	Average pore (nm)
WB	93.00	0.1126	4.843
CAWB	57.08	0.0759	5.319

Adsorption studies

Effect of pyrolysis temperature

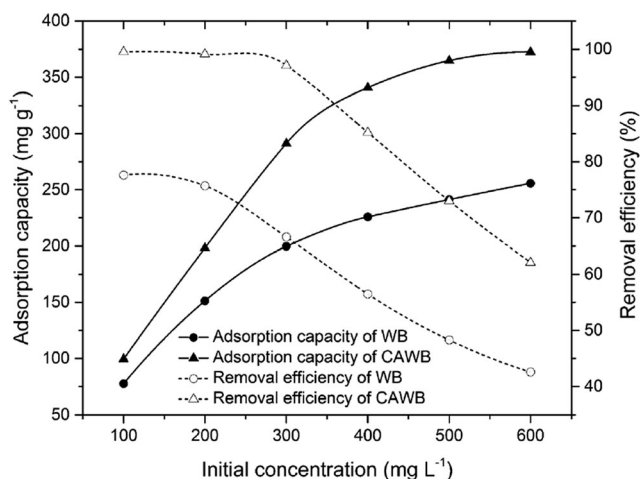
The effect of pyrolysis temperature on the removal efficiency of MB onto WB and CAWB is shown in Table 2. As shown in Table 2, the removal efficiency of MB onto WB decreased from 65.7 to 37.0 % with increasing pyrolysis temperature from 300 to 500 °C, mainly due to the decrease of polar functional groups such as hydroxyl and carboxyl on the surface of WB (Kim et al. 2013). These decreased hydroxyl groups on the surface of WB at higher pyrolysis temperature led to fewer introductions of additional carboxyl groups to the surface of WB via less esterification reaction with carboxyl anhydrides dehydrated from CA, causing a decrease of MB removal efficiency from 99.1 to 61.1 %. This result verified that the introduced carboxyl groups played an important role in the removal of MB by CAWB.

Effect of initial MB concentration

The effects of initial MB concentration on the adsorption capacity and removal efficiency of MB onto WB and CAWB are displayed in Fig. 6. It could be found from Fig. 6 that the adsorption capacity and removal efficiency of the WB were significantly improved after CA treatment. This was due to the introduction of carboxyl groups by CA modification, which could serve as additional sites for MB adsorption onto the biochar surface. With the increase of initial MB concentration from 100 to 600 mg L^{-1} , the amount of MB removed by CAWB at equilibrium increased from 99.5 to 372.4 mg g^{-1} , while the MB removal efficiency showed an opposite trend and decreased from 99.5 to 62.1 %. A higher initial MB concentration could provide a significant driving force to overcome the transfer resistances of MB between the solid and aqueous, which could explain the positive relationship between the amount of MB adsorbed by CAWB at equilibrium

Table 2 Effect of pyrolysis temperature on MB adsorption efficiency of WB and CAWB

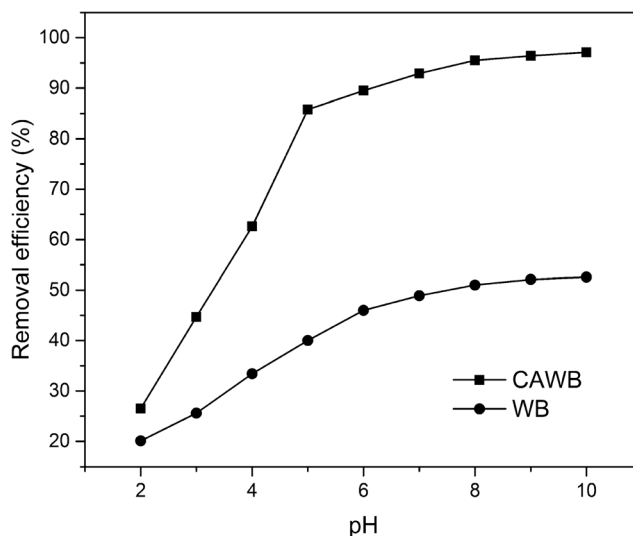
Pyrolysis temperature	300 °C	400 °C	500 °C
WB	65.7 %	46.7 %	37.0 %
CAWB	99.1 %	71.3 %	61.1 %

**Fig. 6** Effect of initial MB concentration on adsorption capacity and removal efficiency of MB onto WB and CAWB

and the initial concentration of MB (Hameed et al. 2008). However, the total available binding sites on the surface of CAWB were limited for certain CAWB dosage; therefore, the MB removal efficiency decreased along with the increase of the initial MB concentration.

Effect of solution pH

The pH of the solution is considered to be an important controlling parameter, which could significantly affect the adsorption process. The analysis of the effect of pH could be a useful tool to investigate the mechanism involved in MB adsorption onto CAWB. The effects of the initial pH of MB solutions on the adsorption of MB onto WB and CAWB are shown in Fig. 7. As seen from Fig. 7, the removal efficiency of CAWB was poor at lower initial pH and increased obviously with the increase of solution pH, then reached the maximum

**Fig. 7** Effect of initial solution pH values on MB removal by WB and CAWB

removal efficiency of 97.07 % at pH 10.0. Thus, the initial solution pH 10.0 was selected for further experiments. At low pH values, the surface of CAWB may be positively charged due to the protonation of the surface functional groups such as hydroxyl and carboxyl groups, which was verified to be the important functional groups involved in the adsorption of MB in the FTIR analysis above. Additionally, the excess H⁺ and H₃O⁺ ions may compete with dye cations (MB⁺) for the same binding sites (Gong et al. 2008). Therefore, the lower adsorption efficiency at low pH was due to the electrostatic repulsion presented between the dye cations and the positively charged surface of CAWB. When the pH of MB solution increased, the competition between the protons and dye cations for the adsorption sites available on CAWB surface was weakened. Moreover, the hydroxyl and carboxyl groups were deprotonated and more binding sites could be released at higher pH value. The electrostatic attraction that occurred between the dye cations and negatively charged surface of CAWB at high pH could account for the increase of MB adsorption onto CAWB. These results indicated that the electrostatic attraction might be an important mechanism for MB removal, which was similar to the conclusions made in previous studies on MB adsorption (Hameed et al. 2008).

Effect of ionic strength

The influence of NaCl concentrations was investigated to determine the effect of background ionic strength of MB adsorption onto CAWB, and the result is shown in Fig. 8. As seen from Fig. 8, it was concluded that the MB adsorption onto CAWB was dependent on the concentration of NaCl because the adsorption efficiency of CAWB decreased from 99.1 to 75.3 % as the concentration of NaCl increased from 0.001 to 0.1 mol L⁻¹. The decrease might be due to the competition of

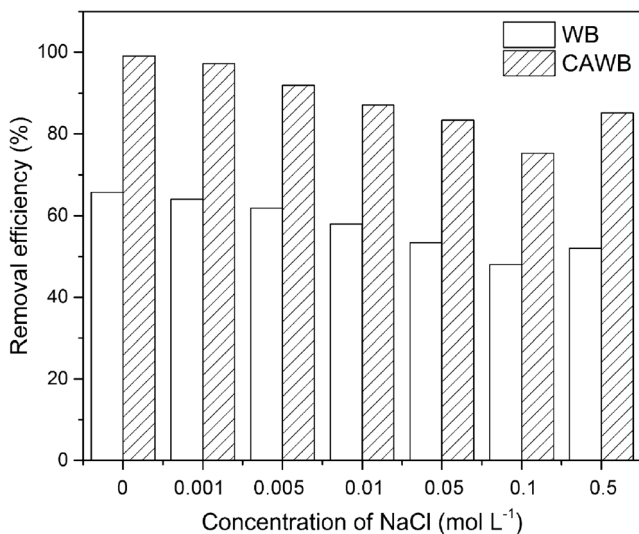


Fig. 8 Effect of different NaCl concentrations on MB removal by WB and CAWB

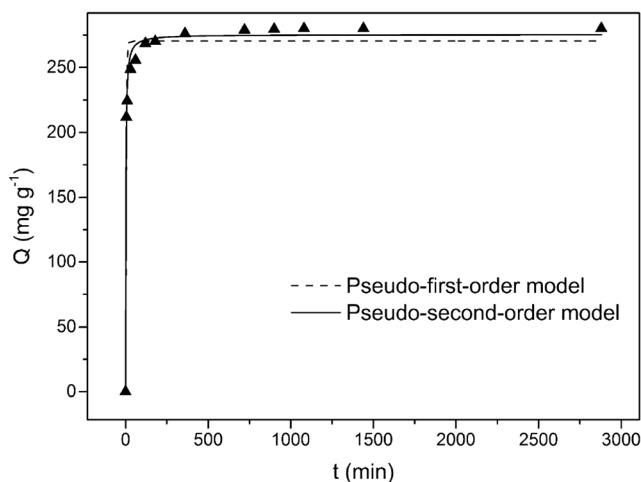


Fig. 9 Kinetics of MB adsorption onto CAWB at 30 °C (volume = 50 mL; initial MB concentration = 300 mg L⁻¹; pH = 10.0, contact time = 5–2880 min)

Na⁺ with the positively charged MB for the same adsorption sites on the negatively charged surface of CAWB. This result confirmed the involvement of electrostatic attraction in the MB adsorption onto CAWB, which was consistent with the analysis of the effect of pH above. However, there existed a slight increase of the adsorption of MB when the NaCl concentration reached 0.5 mol L⁻¹ in comparison with 0.1 mol L⁻¹, which might be due to the aggregation of MB molecules induced by salt ions (Ma et al. 2012).

Adsorption kinetics

The effect of contact time on MB removal by CAWB is displayed in Fig. 9. As seen from Fig. 9, the adsorption of MB by CAWB was rapid within the first 60 min, and it should be noted that over 70 and 90 % of the total MB was removed at the time of 5 and 60 min, respectively. The rapid adsorption in this stage may be attributed to the sufficient active binding sites on the surface of CAWB. After the rapid adsorption stage, the removal rate decreased gradually and achieved equilibrium after 12 h.

Both pseudo-first-order and pseudo-second-order models were applied to investigate the adsorption mechanism of MB onto CAWB. The two models could be expressed by the following equations respectively:

$$q_t = q_e(1 - e^{-k_1 t}) \tag{1}$$

Table 3 Kinetic parameters for adsorption of MB onto CAWB

Pseudo-first-order			Pseudo-second-order		
$q_{e,1}$ (mg g ⁻¹)	k_1 (min ⁻¹)	R^2	$q_{e,2}$ (g mg ⁻¹ min) ⁻¹	k_2 (min ⁻¹)	R^2
270.35	0.262	0.97	275.35	0.002	0.99

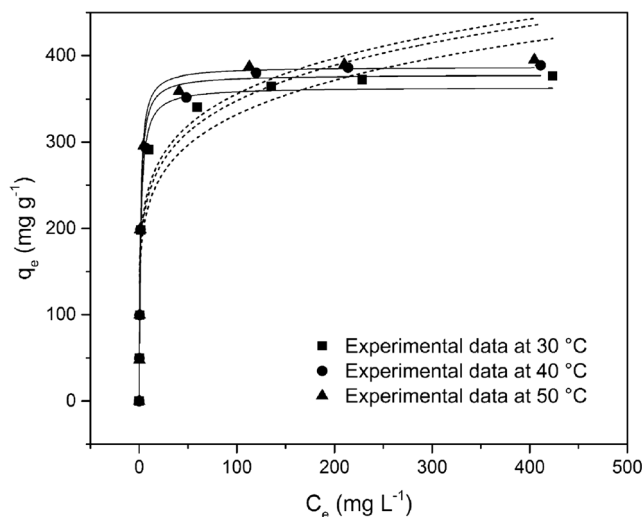


Fig. 10 Langmuir isotherm (solid line) and Freundlich isotherm (dash line) for the adsorption of MB onto CAWB (MB solution volume = 50 mL; adsorbent dose = 50 mg; initial MB concentration = 50–800 mg L⁻¹; pH = 10.0; contact time = 24 h; $T = 30, 40, 50$ °C)

$$q_t = \frac{k_2 q_e^2 t}{1 + k_2 q_2 t} \quad (2)$$

where q_e and q_t are used to represent the amount of MB removed by CAWB at equilibrium and time t , respectively (mg g⁻¹), and k_1 and k_2 are the adsorption rate constants (min⁻¹) of the first order and second order, respectively. These parameters of two kinetic models as mentioned above are summarized in Table 3.

As could be obviously seen from Table 3 that the experimental data in this study were better fitted by the pseudo-second-order model ($R^2 = 0.99$) than the pseudo-first-order model ($R^2 = 0.97$). Additionally, the value q_e (275.35 mg g⁻¹) calculated by the pseudo-second-order model was more equal to the experimental value (280.10 mg g⁻¹) than the pseudo-first-order one (270.35 mg g⁻¹). The fact that the pseudo-second-order model was more suitable for describing MB adsorption process indicated that the removal of MB by CAWB was dominated by chemisorption, involving chelating reaction and ion exchange between the adsorbent and adsorbate (Sun et al. 2013).

Adsorption isotherms

Adsorption isotherms are significant in describing how the adsorbate interacts with adsorbents, which are critical for us to optimize the use of adsorbents. To better explain the equilibrium characteristics of the MB adsorption onto CAWB, Langmuir (Eq. (3) and Eq. (4)) and Freundlich (Eq. (5)) isotherm models were applied to simulate the experimental data. Their governing equations are expressed as follows:

$$q_e = \frac{q_m K_L c_e}{1 + K_L c_e} \quad (3)$$

$$R_L = \frac{1}{1 + K_L c_0} \quad (4)$$

$$q_e = K_F c_e^{1/n} \quad (5)$$

where c_0 and c_e are the initial and equilibrium concentrations of MB in aqueous solution (mg L⁻¹), and q_m denotes the maximum adsorption capacity obtained from Langmuir model. K_L is the Langmuir equilibrium constant related to interaction energies (L mg⁻¹). R_L , as the dimensionless constant separation factor of Langmuir equation, is used to indicate whether the adsorption equilibrium is favorable ($0 < R_L < 1$) or unfavorable ($R_L > 1$). K_F and n denote the Freundlich affinity coefficient and Freundlich linearity constant.

The equilibrium isotherms for MB adsorption by CAWB at different temperatures (30, 40, and 50 °C) are displayed in Fig. 10. The relative isotherm parameters are shown in Table 4. As seen from Table 4, the Langmuir model has better R^2 values (0.992, 0.992, and 0.995) than the Freundlich model (0.850, 0.832, and 0.808) at all temperatures, which was consistent with the previous researches (Zeng et al. 2015). The result confirmed the monolayer coverage of MB and the homogenous distribution of a finite number of active binding sites on the surface of CAWB (Yao et al. 2013). The values R_L in the adsorption of MB by CAWB at all temperatures (0.0019, 0.0016, and 0.0015) were less than 1 and greater than 0, which verified that the adsorption process of MB onto CAWB was favorable. Moreover, the K_L value increased with the increase in temperature, which was related to the affinity of binding sites, indicating that the MB adsorption onto CAWB was an endothermic process and it was favorable for the adsorption at higher temperature due to the increase in

Table 4 Langmuir and Freundlich isotherm parameters for adsorption of MB onto CAWB

T (°C)	Langmuir model			Freundlich model			
	q_m (mg g ⁻¹)	K_L (L mg ⁻¹)	R^2	R_L	K_F (L mg ⁻¹)	n	R^2
30 °C	84.87	0.02	0.992	0.0019	11.28	3.03	0.850
40 °C	94.38	0.03	0.992	0.0016	14.79	3.23	0.832
50 °C	96.18	0.10	0.995	0.0015	25.35	4.01	0.808

Table 5 Comparison of the maximum MB adsorption capacity of various adsorbents

Adsorbents	Adsorption capacity (mg g ⁻¹)	References
CAWB	395	This study
Rice husk activated carbon	343.5	Kannan and Sundaram (2001)
Rattan sawdust activated carbon	294.12	Hameed et al. (2007)
Graphene-coated cotton wood biochar	174	Zhang et al. (2012)
Cationic surfactant-modified water hyacinth biochar	103.2	Sumanjit et al. (2015)

collision frequency between CAWB and MB (Sumanjit et al. 2015). Nevertheless, there exists little difference between the calculated maximum adsorption capacities at different temperatures, which indicated that CAWB could also be an effective adsorbent in aqueous solution at relatively low temperature. Table 5 summarizes the maximum adsorption capacity of CAWB with various adsorbents in previous studies. As could be seen from Table 5, CAWB showed an excellent MB removal ability compared to many other adsorbents (Hameed et al. 2007; Kannan and Sundaram 2001; Sumanjit et al. 2015; Zhang et al. 2012).

Thermodynamic analysis

Whether adsorption was endothermic or exothermic could be defined by thermodynamic parameters such as enthalpy ΔH^0 , entropy ΔS^0 , and Gibbs free energy ΔG^0 . These parameters could be obtained by the following equations:

$$\Delta G^0 = -RTK^0 \tag{6}$$

$$\ln k^0 = \frac{\Delta H^0}{RT} + \frac{\Delta S^0}{R} \tag{7}$$

where R is the gas constant 8.314 J mol⁻¹ K⁻¹, T (K) is the absolute temperature in Kelvin, and K^0 could be calculated by plotting $\ln(q_e/c_e)$ versus c_e and extrapolating c_e to zero. From the linear plot of ΔG^0 , the values of ΔH^0 (kJ mol⁻¹) and ΔS^0 (kJ mol⁻¹ K⁻¹) could be obtained from the slope and intercept.

In this study, the adsorption experiments were carried out at different absolute temperatures of 303.15 K (30 °C), 313.15 K (40 °C), and 323.15 K (50 °C). The results of thermodynamic studies are shown in Table 6. The negative value of ΔG^0 at all temperatures verified the feasibility and spontaneous nature of the MB adsorption process onto CAWB. Furthermore, when the temperature increased from 30 to 50 °C, the Gibbs free

energy ΔG^0 decreased from -3.546 to -3.931 kJ mol⁻¹, indicating that the adsorption process was more spontaneous at higher temperature (Gan et al. 2015).

The positive value of ΔH^0 (2.284 kJ mol⁻¹) verified the endothermic nature of the adsorption of MB onto CAWB, which was consistent with the above conclusions of adsorption isotherms analysis. The positive value of ΔS^0 reflected the affinity of the CAWB for MB and suggested the increase of randomness at the solid-solution interface during the MB adsorption process (Kołodzyńska et al. 2012). We could draw the conclusion that the MB adsorption onto CAWB was an endothermic and spontaneous process, which was consistent with the results obtained in the adsorption isotherms study.

Regeneration analysis

Regeneration of exhausted adsorbent could make the treatment process more economical and sustainable. To realize the regeneration, 0.1 mol L⁻¹ HCl was used as the eluent to desorb the MB loaded on CAWB in this study. It could be seen from Fig. 11 that the eluent performed well in desorbing the adsorbed MB, verifying the electrostatic attraction mechanism of MB adsorption, since HCl could corrupt these bonds between dye cations and negatively charged surface of CAWB (Dotto et al. 2015). Furthermore, the removal efficiency of MB onto reused CAWB was still over 85 % at the fifth cycle, after decreasing gradually from 97.1 % with the increase of cycles. The decreasing tendency of the removal efficiency may due to the weakness of polar functional groups and the decrease of specific surface area of CAWB (Gan et al. 2015). After multiple cycle adsorptions, the CAWB still exhibited an excellent regeneration and adsorption performance, indicating that the adsorbent could be used as a cost-effective adsorbent for dyes decontamination.

Table 6 Thermodynamic parameters for MB adsorption onto CAWB

ln k^0			ΔG^0 (kJ mol ⁻¹)			ΔH^0 (kJ mol ⁻¹)	ΔS^0 (kJ mol ⁻¹ K ⁻¹)	R^2
30 °C	40 °C	50 °C	30 °C	40 °C	50 °C			
1.407	1.442	1.463	-3.546	-3.754	-3.931	2.284	19.25	0.99

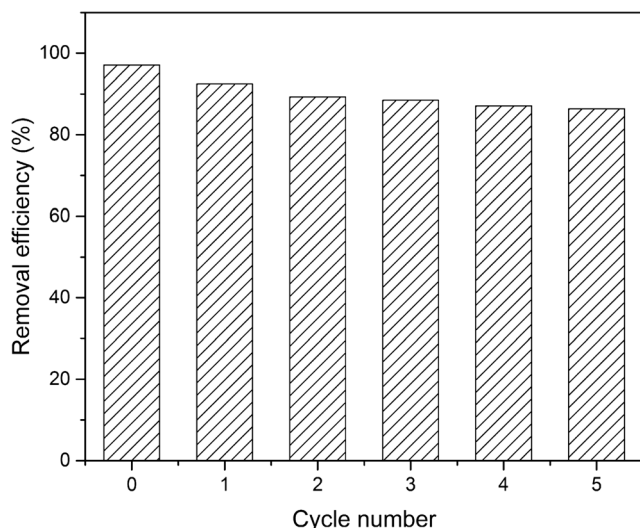


Fig. 11 Five sequential adsorption-desorption cycles of CAWB for MB removal (volume = 50 mL; adsorbent dose = 50 mg; initial MB concentration = 300 mg L⁻¹; pH = 10.0; contact time = 24 h; T = 30 °C)

Application of CAWB to actual dye wastewater

To realize the environmental application of CAWB, it is vital to demonstrate the adsorption efficiency of the adsorbent to real dye wastewater. We compared the treatment effects of CAWB on wastewater and MB solutions prepared with ultrapure water and river water. The results are shown in Table 7. It could be found that the adsorption capacity for MB in real wastewater onto CAWB (228.1 mg L⁻¹) was slightly lower than that of MB in ultrapure water (234.8 mg L⁻¹) and river water (232.2 mg L⁻¹) but still reflected a high removal ability to the MB in aqueous solution. The slight decrease in adsorption capacity of MB in real industrial effluent may be attributed to the competition of adsorption sites available on CAWB surface between MB cations and some other contaminants or inorganic ions present in the wastewater, such as Na⁺ (Kaushik and Malik 2013). It could be seen from Table 7 that CAWB exhibited a high adsorption capacity in the removal of MB in the real dye wastewater, which verified its feasibility of environmental application in the dye wastewater treatment. In the disposal of dye-contaminated effluent by CAWB, the widespread and overgrown water hyacinth could be used as a sufficient feedstock for biochar preparation. CA modification of water hyacinth biochar after pyrolyzing at 300 °C

Table 7 Comparison of the treatment effects of CAWB in various water samples

Water samples	Adsorption capacity (mg g ⁻¹)	Removal efficiency
Dye wastewater	228.1	96.7 %
River water	232.3	98.4 %
Ultrapure water	234.8	99.5 %

could greatly enhance the MB adsorption capacity of the adsorbent with low energy consumption. The excellent reusability of the CA-modified biochar may further reduce the application cost. Consequently, CAWB demonstrated a great potential in the decontamination of dye wastewater.

Conclusions

A novel effective adsorbent was successfully prepared via CA modification of water hyacinth biomass-derived biochar, which demonstrated an excellent ability to remove MB in aqueous solution. The mechanism of MB adsorption onto CAWB involved the specific interactions between hydroxyl and carboxyl groups on the surface of CAWB with MB molecules, and electrostatic attraction between the dye cations and negatively charged surface of CAWB. CA modification could significantly enhance the MB removal ability of biochar by increasing the adsorption sites on the surface of the biochar due to the introduction of additional carboxyl via esterification reaction. Furthermore, the removal capacity could also be enhanced by the increase of initial MB concentration, solution pH, and temperature. The adsorption process of MB onto CAWB was better fitted by the pseudo-second-order kinetic model and Langmuir adsorption model. The exhausted adsorbent could be effectively regenerated by 0.1 mol L⁻¹ HCl and maintain ideal removal ability to MB after multiple cycle adsorptions. When applied in the removal of MB in the actual dye wastewater, CAWB still exhibited a high adsorption efficiency. We believe that the CA-modified biochar derived from water hyacinth could be a new cost-effective and environment-friendly adsorbent for wide utilization in dye removal. To realize the more extensive application of this adsorbent, the investigations of its adsorption efficiency to other contaminants are needed in our further research.

Acknowledgments The study was financially supported by the National Natural Science Foundation of China (grant no. 41271332, 51478470, and 51521006) and the Hunan Provincial Innovation Foundation for Postgraduate (grant no. CX2015B090).

References

- Ahmad M, Lee SS, Dou X, Mohan D, Sung JK, Yang JE, Ok YS (2012) Effects of pyrolysis temperature on soybean stover- and peanut shell-derived biochar properties and TCE adsorption in water. *Bioresour Technol* 118:536–544
- Ahmad M, Rajapaksha AU, Lim JE, Zhang M, Bolan N, Mohan D, Vithanage M, Lee SS, Ok YS (2014) Biochar as a sorbent for contaminant management in soil and water: a review. *Chemosphere* 99: 19–33
- Annadurai GJR, Lee DJ (2002) Use of cellulose-based wastes for adsorption of dyes from aqueous solutions. *J Hazard Mater B* 92:263–274

- Auta M, Hameed BH (2012) Modified mesoporous clay adsorbent for adsorption isotherm and kinetics of methylene blue. *Chem Eng J* 198:199:219–227
- Burhenne L, Aicher T (2014) Benzene removal over a fixed bed of wood char: the effect of pyrolysis temperature and activation with CO₂ on the char reactivity. *Fuel Process Technol* 127:140–148
- Chen JP, Wu S, Chong K-H (2003) Surface modification of a granular activated carbon by citric acid for enhancement of copper adsorption. *Carbon* 41:1979–1986
- Chen B, Chen Z, Lv S (2011a) A novel magnetic biochar efficiently sorbs organic pollutants and phosphate. *Bioresour Technol* 102:716–723
- Chen X, Chen G, Chen L, Chen Y, Lehmann J, McBride MB, Hay AG (2011b) Adsorption of copper and zinc by biochars produced from pyrolysis of hardwood and corn straw in aqueous solution. *Bioresour Technol* 102:8877–8884
- Cope CO, Webster DS, Sabatini DA (2014) Arsenate adsorption onto iron oxide amended rice husk char. *Sci Total Environ* 488–489:554–561
- Dong X, Ma LQ, Li Y (2011) Characteristics and mechanisms of hexavalent chromium removal by biochar from sugar beet tailing. *J Hazard Mater* 190:909–915
- Dotto GL, Santos JM, Rodrigues IL, Rosa R, Pavan FA, Lima EC (2015) Adsorption of Methylene Blue by ultrasonic surface modified chitin. *J Colloid Interf Sci* 446:133–140
- Feng Y, Zhou H, Liu G, Qiao J, Wang J, Lu H, Yang L, Wu Y (2012) Methylene blue adsorption onto swede rape straw (*Brassica napus* L.) modified by tartaric acid: equilibrium, kinetic and adsorption mechanisms. *Bioresour Technol* 125:138–144
- Gan C, Liu Y, Tan X, Wang S, Zeng G, Zheng B, Li T, Jiang Z, Liu W (2015) Effect of porous zinc–biochar nanocomposites on Cr(vi) adsorption from aqueous solution. *RSC Adv* 5:35107–35115
- Gong R, Zhong K, Hu Y, Chen J, Zhu G (2008) Thermochemical esterifying citric acid onto lignocellulose for enhancing methylene blue sorption capacity of rice straw. *J Environ Manag* 88:875–880
- Gulnaz O, Kaya A, Matyar F, Arikian B (2004) Sorption of basic dyes from aqueous solution by activated sludge. *J Hazard Mater* 108:183–188
- Hameed BH, Ahmad AL, Latiff KNA (2007) Adsorption of basic dye (methylene blue) onto activated carbon prepared from rattan sawdust. *Dyes Pigments* 75:143–149
- Hameed BH, Mahmoud DK, Ahmad AL (2008) Sorption equilibrium and kinetics of basic dye from aqueous solution using banana stalk waste. *J Hazard Mater* 158:499–506
- Harikishore Kumar Reddy D, Lee S-M (2014) Magnetic biochar composite: facile synthesis, characterization, and application for heavy metal removal. *Colloid Surface A* 454:96–103
- Inyang M, Gao B, Zimmerman A, Zhang M, Chen H (2014) Synthesis, characterization, and dye sorption ability of carbon nanotube–biochar nanocomposites. *Chem Eng J* 236:39–46
- Jing X-R, Wang Y-Y, Liu W-J, Wang Y-K, Jiang H (2014) Enhanced adsorption performance of tetracycline in aqueous solutions by methanol-modified biochar. *Chem Eng J* 248:168–174
- Kannan N, Sundaram MM (2001) Kinetics and mechanism of removal of methylene blue by adsorption on various carbons—a comparative study. *Dyes Pigments* 51:25–40
- Kaushik P, Malik A (2013) Comparative performance evaluation of *Aspergillus lentulus* for dye removal through bioaccumulation and biosorption. *Environ Sci Pollut R* 20:2882–2892
- Kim WK, Shim T, Kim YS, Hyun S, Ryu C, Park YK, Jung J (2013) Characterization of cadmium removal from aqueous solution by biochar produced from a giant *Miscanthus* at different pyrolytic temperatures. *Bioresour Technol* 138:266–270
- Kołodnyńska D, Wnętrzak R, Leahy JJ, Hayes MHB, Kwapiński W, Hubicki Z (2012) Kinetic and adsorptive characterization of biochar in metal ions removal. *Chem Eng J* 197:295–305
- Kong L, Xiong Y, Sun L, Tian S, Xu X, Zhao C, Luo R, Yang X, Shih K, Liu H (2014) Sorption performance and mechanism of a sludge-derived char as porous carbon-based hybrid adsorbent for benzene derivatives in aqueous solution. *J Hazard Mater* 274:205–211
- Leyva-Ramos R, Landin-Rodriguez LE, Leyva-Ramos S, Medellin-Castillo NA (2012) Modification of corncob with citric acid to enhance its capacity for adsorbing cadmium(II) from water solution. *Chem Eng J* 180:113–120
- Low KS, Lee CK, Mak SM (2004) Sorption of copper and lead by citric acid modified wood. *Wood Sci Technol* 38:629–640
- Ma J, Yu F, Zhou L, Jin L, Yang M, Luan J, Tang Y, Fan H, Yuan Z, Chen J (2012) Enhanced adsorptive removal of methyl orange and methylene blue from aqueous solution by alkali-activated multiwalled carbon nanotubes. *ACS Appl Mater Inter* 4:5749–5760
- Mahmoud DK, Salleh MAM, Karim WAWA, Idris A, Abidin ZZ (2012) Batch adsorption of basic dye using acid treated kenaf fibre char: equilibrium, kinetic and thermodynamic studies. *Chem Eng J* 181–182:449–457
- Malik A (2007) Environmental challenge vis a vis opportunity: the case of water hyacinth. *Environ Int* 33:122–138
- Mao J, Won SW, Vijayaraghavan K, Yun Y-S (2010) Immobilized citric acid-treated bacterial biosorbents for the removal of cationic pollutants. *Chem Eng J* 162:662–668
- Marshall WEWL, Boler DE, Johns MM, Toles CA (1999) Enhanced metal adsorption by soybean hulls modified with citric acid. *Bioresour Technol* 69:263–268
- Masto RE, Kumar S, Rout TK, Sarkar P, George J, Ram LC (2013) Biochar from water hyacinth (*Eichornia crassipes*) and its impact on soil biological activity. *Catena* 111:64–71
- Pitsari S, Tsoufakis E, Loizidou M (2013) Enhanced lead adsorption by unbleached newspaper pulp modified with citric acid. *Chem Eng J* 223:18–30
- Qian L, Chen B (2014) Interactions of aluminum with biochars and oxidized biochars: implications for the biochar aging process. *J Agr Food Chem* 62:373–380
- Sajab MS, Chia CH, Zakaria S, Jani SM, Ayob MK, Chee KL, Khiew PS, Chiu WS (2011) Citric acid modified kenaf core fibres for removal of methylene blue from aqueous solution. *Bioresour Technol* 102:7237–7243
- Shen YS, Wang SL, Tzou YM, Yan YY, Kuan WH (2012) Removal of hexavalent Cr by coconut coir and derived chars—the effect of surface functionality. *Bioresour Technol* 104:165–172
- Sumanjit S, Mahajan RK, Gupta VK (2015) Modification of surface behaviour of *Eichhornia crassipes* using surface active agent: an adsorption study. *Journal of J Ind Eng Chem* 21:189–197
- Sun L, Wan S, Luo W (2013) Biochars prepared from anaerobic digestion residue, palm bark, and eucalyptus for adsorption of cationic methylene blue dye: characterization, equilibrium, and kinetic studies. *Bioresour Technol* 140:406–413
- Tan X, Liu Y, Zeng G, Wang X, Hu X, Gu Y, Yang Z (2015) Application of biochar for the removal of pollutants from aqueous solutions. *Chemosphere* 125:70–85
- Wang B, Li C, Liang H (2013a) Bioleaching of heavy metal from woody biochar using *Acidithiobacillus ferrooxidans* and activation for adsorption. *Bioresour Technol* 146:803–806
- Wang S, Wang L, Kong W, Ren J, Liu C, Wang K, Sun R, She D (2013b) Preparation, characterization of carboxylated bamboo fibers and their adsorption for lead(II) ions in aqueous solution. *Cellulose* 20:2091–2100
- Wang H, Yuan X, Zeng G, Leng L, Peng X, Liao K, Peng L, Xiao Z (2014) Removal of malachite green dye from wastewater by different organic acid-modified natural adsorbent: kinetics, equilibriums, mechanisms, practical application, and disposal of dye-loaded adsorbent. *Environ Sci Pollut R* 21:11552–11564
- Tong X-j, Li J-y, Yuan J-h, Xu R-k (2011) Adsorption of Cu(II) by biochars generated from three crop straws. *Chem Eng J* 172:828–834

- Yagub MT, Sen TK, Afroze S, Ang HM (2014) Dye and its removal from aqueous solution by adsorption: a review. *Adv Colloid Interface* 209:172–184
- Yang J, Qiu K (2010) Preparation of activated carbons from walnut shells via vacuum chemical activation and their application for methylene blue removal. *Chem Eng J* 165:209–217
- Yao Y, Gao B, Chen J, Yang L (2013) Engineered biochar reclaiming phosphate from aqueous solutions: mechanisms and potential application as a slow-release fertilizer. *Environ Sci Technol* 47:8700–8708
- Zeng L, Xie M, Zhang Q, Kang Y, Guo X, Xiao H, Peng Y, Luo J (2015) Chitosan/organic rectorite composite for the magnetic uptake of methylene blue and methyl orange. *Carbohydr Polym* 123:89–98
- Zhang Z, Zhang Z, Fernández Y, Menéndez JA, Niu H, Peng J, Zhang L, Guo S (2010) Adsorption isotherms and kinetics of methylene blue on a low-cost adsorbent recovered from a spent catalyst of vinyl acetate synthesis. *Appl Surf Sci* 256:2569–2576
- Zhang M, Gao B, Yao Y, Xue Y, Inyang M (2012) Synthesis, characterization, and environmental implications of graphene-coated biochar. *Sci Total Environ* 435–436:567–572
- Zhou Y, Gu X, Zhang R, Lu J (2014) Removal of aniline from aqueous solution using pine sawdust modified with citric acid and β -cyclodextrin. *Ing Eng Chem Res* 53:887–894
- Zou W, Zhao L (2011) Removal of uranium(VI) from aqueous solution using citric acid modified pine sawdust: batch and column studies. *J Radioanal Nucl Ch* 292:585–595
- Zou W, Bai H, Gao S, Li K (2013) Characterization of modified sawdust, kinetic and equilibrium study about methylene blue adsorption in batch mode. *Korean J Chem Eng* 30:111–122